Protein Engineering, Design & Selection, 2016, vol. 29 no. 6, pp. 197–207
doi: 10.1093/protein/gzw007
Advance Access Publication Date: 19 April 2016
Original Article

Original Article

Binding of the substrate UDP-glucuronic acid induces conformational changes in the xanthan gum glucuronosyltransferase

S.R. Salinas[1,4], A.A. Petruk[2,3,5], N.G. Brukman[1,6], M.I. Bianco[1,7], M. Jacobs[1], M.A. Marti[3], and L. Ielpi[1,*]

[1]Laboratory of Bacterial Genetics, Fundación Instituto Leloir, IIBBA-CONICET, Av. Patricias Argentinas 435, C1405BWE Buenos Aires, Argentina, [2]Departamento de Química Inorgánica, Analítica, y Química Física/ INQUIMAE CONICET, Córdoba, Argentina, and [3]Departamento de Química Biológica, Facultad de Ciencias Exactas y Naturales, Universidad de Buenos Aires, Ciudad Universitaria, Pabellón 2, C1428EHA Buenos Aires, Argentina

*To whom correspondence should be addressed. Fundación Instituto Leloir. C1405BWE – Buenos Aires, Argentina.
E-mail: lielpi@leloir.org.ar
[4]Present address: Departamento de Química Biológica, CIQUIBIC-CONICET, Universidad Nacional de Córdoba, Argentina.
[5]Present address: Department of Chemistry, Faculty of Science, University of Waterloo, Waterloo, Ontario, Canada.
[6]Present address: IBYME-CONICET, Buenos Aires, Argentina.
[7]Present address: Instituto de Ciencia y Tecnología Dr. César Milstein, Fundación Pablo Cassará-CONICET, Buenos Aires, Argentina.
Edited by Stephen Withers

Received 1 October 2015; Revised 21 January 2016; Accepted 2 March 2016

Abstract

GumK is a membrane-associated glucuronosyltransferase of *Xanthomonas campestris* that is involved in xanthan gum biosynthesis. GumK belongs to the inverting GT-B superfamily and catalyzes the transfer of a glucuronic acid (GlcA) residue from uridine diphosphate (UDP)-GlcA (UDP-GlcA) to a lipid-PP-trisaccharide embedded in the membrane of the bacteria. The structure of GumK was previously described in its apo- and UDP-bound forms, with no significant conformational differences being observed. Here, we study the behavior of GumK toward its donor substrate UDP-GlcA. Turbidity measurements revealed that the interaction of GumK with UDP-GlcA produces aggregation of protein molecules under specific conditions. Moreover, limited proteolysis assays demonstrated protection of enzymatic digestion when UDP-GlcA is present, and this protection is promoted by substrate binding. Circular dichroism spectroscopy also revealed changes in the GumK tertiary structure after UDP-GlcA addition. According to the obtained emission fluorescence results, we suggest the possibility of exposure of hydrophobic residues upon UDP-GlcA binding. We present *in silico*-built models of GumK complexed with UDP-GlcA as well as its analogs UDP-glucose and UDP-galacturonic acid. Through molecular dynamics simulations, we also show that a relative movement between the domains appears to be specific and to be triggered by UDP-GlcA. The results presented here strongly suggest that GumK undergoes a conformational change upon donor substrate binding, likely bringing the two Rossmann fold domains closer together and triggering a change in the N-terminal domain, with consequent generation of the acceptor substrate binding site.

Key words: conformational change, glycosyltransferase, GumK, membrane monotopic protein, xanthan

Introduction

Glycosyltransferases (GTs) are enzymes that catalyze the specific transfer of a sugar moiety from nucleotide sugar or lipid-phospho-sugar donors to a wide range of acceptor substrates, including mono-, oligo- and polysaccharides, lipids, proteins, small organic molecules and deoxyribonucleic acids (Lairson *et al.*, 2008). GTs are the most abundant enzymes on earth and participate in a wide variety of biological processes (Coutinho *et al.*, 2003; Weadge *et al.*, 2007). The Carbohydrate Active Enzymes database (CAZy, http://www.cazy.org) groups more than 200 000 GTs into 97 families based on sequence similarity (Lombard *et al.*, 2014). Despite the relatively low sequence identity among GTs, the nucleotide sugar-dependent GTs present two principal folds: GT-A and GT-B (Henrissat *et al.*, 2008; Breton *et al.*, 2012). Both of these folds contain Rossmann fold domains, but they also exhibit several differences. In general, the GT-A superfamily, but not GT-B, binds a divalent metal ion, which is required for enzyme activity. The GT-B superfamily contains two Rossmann fold domains, forming a deep cleft that constitutes the active site. In GT-B enzymes, the interaction of the donor substrate occurs mainly with the C-terminal domain, while the N-terminal domain is involved in acceptor binding.

GumK is an inverting GT member of CAZy family 70, which is involved in the biosynthesis of the exopolysaccharide xanthan by the bacteria *Xanthomonas campestris*. Specifically, GumK transfers a glucuronic acid (GlcA) residue from uridine diphosphate (UDP)-GlcA to the mannose-α-1,3-glucose-β-1,4-glucose-diphosphate-polyisoprenyl acceptor (Lip-PP-trisaccharide) during the biosynthesis of the pentasaccharidic subunit of xanthan (Katzen *et al.*, 1998; Barreras *et al.*, 2008). GumK is a membrane monotopic protein, belonging to the special group of membrane-associated GT-B, that is highly specific for UDP-GlcA as a sugar donor, and the lipid portion of the acceptor substrate is essential for enzymatic transfer (Barreras *et al.*, 2004). In previous studies from our group, we solved the crystallographic structure of apo-GumK (PDB ID: 2HY7) at a 1.9 Å resolution, revealing a GT-B fold (Barreras *et al.*, 2006, 2008). Crystals could not be obtained in co-crystallization assays between GumK and UDP-GlcA. Only the UDP portion of UDP-GlcA was detected in soaking experiments (PDB ID: 2Q6V). No significant structural deviation was observed between apo- and UDP-bound GumK [root mean square deviation (RMSD) 0.46 Å, Cα, 370 residues]. Through *in vitro* enzymatic assays, we observed that GumK is able to hydrolyze UDP-GlcA in the absence of the acceptor substrate. Therefore, for avoiding UDP-GlcA hydrolysis, we identified and crystallized a non-active and non-hydrolytic GumK, GumKD157A (PDB ID: 3CUY). By soaking the crystals with UDP-GlcA, we also obtained a GumKD157A/UDP complex (PDB ID: 3CV3) with exactly the same UDP location and conformation observed for wild-type GumK/UDP crystals. The absence of electron density corresponding to GlcA even in the non-hydrolytic GumKD157A provided the first hint of the probable existence of a dynamic process upon UDP-GlcA binding instead of UDP-GlcA hydrolysis. We also found that the N-terminal domain of GumK exhibits a basic *pI* of 9.97 and that the electrostatic surface potential displays a patch of basic and hydrophobic residues in this domain (Fig. 1A) (Barreras *et al.*, 2008). The patch comprises residues in helices Nα2 (R55-K60) and Nα4 (S97-A112) and in the linker region between Nα4 and Nβ4 (W85-R96). We therefore hypothesized that this cluster may be involved in acceptor substrate and membrane binding, which is a mechanism that has been proposed for several membrane GTs (Ha *et al.*, 2000; Edman *et al.*, 2003; Grizot *et al.*, 2006; Guerin *et al.*, 2007; Lind *et al.*, 2007).

As there are few unexpected features in the nucleotide sugar-dependent GT folds, it appears that the mechanisms of binding and catalysis may account for the large variety of substrates found among GTs. The biochemical characteristics of GumK have been studied previously, but the molecular mechanism of sugar-nucleotide binding remains unclear and is poorly described as it is for the majority of GTs. In recent years, some evidence has been obtained regarding the conformational changes that occur upon substrate binding in GTs of the GT-B superfamily (Albesa-Jove *et al.*, 2014). Examples include the enzyme involved in mycothiol synthesis in *Corynebacterium glutamicum*, MshA, which brings together both domains with 97° of relative rotation after UDP-GlcNac binding, thus generating the acceptor binding site, as observed via crystallography (Vetting *et al.*, 2008). Another example is the well-studied α-mannosyltransferase PimA protein from *Mycobacterium smegmatis*. PimA catalyzes the transfer of mannose from GDP-Man to phosphatidyl-myo-inositol. After GDP binding, PimA is stabilized and compacted in a 'closed' conformation. This closure is proposed as a mechanism for the structural organization of a functionally active site. In contrast, the addition of phosphatidyl-myo-inositol to apo- or GDP-bound PimA leads to a less compact structure with a lower melting temperature compared with the apo- and GDP-bound forms. The authors demonstrated that particular regions in the N-terminal domain of PimA display conformational flexibility and secondary structure reshuffling, which is responsible for the conformational behavior of the enzyme (Giganti *et al.*, 2013, 2015). This conformational flexibility is also present in members of the GT-A family. It has recently been demonstrated that the lipopolysaccharide α-1,4-galactosyltransferase C from *Neisseria meningitidis*, LgtC, adopts multiple interconverting conformational states (Chan *et al.*, 2012). In general, dynamic processes are considered to be the fourth dimension of protein structure, and elucidating these processes permits a better understanding of protein function to be obtained (Hubbell *et al.*, 2000; Mittermaier and Kay, 2009; McHaourab *et al.*, 2011).

The future challenges in the study of membrane-associated GT-B proposed by Albesa-Jové *et al.* (Albesa-Jove *et al.*, 2014) include the understanding of its dynamics and conformational changes. Here, we present the first insight on the behavior of membrane-associated GumK, the only member of GT-70 with known structure, toward its donor substrate. Using several biochemical and biophysical methods, such as absorption spectroscopy and limited proteolysis, we investigated the existence of conformational changes in GumK triggered by specific UDP-GlcA binding. Herein, we describe the modeling of the donor substrate UDP-GlcA in GumK via molecular docking. Based on comparing the models of GumK with UDP-GlcA and with the non-substrate sugar nucleotides UDP-Glc and UDP-GalA, we propose several interactions that may account for UDP-GlcA specificity. In addition, a slight conformational change in GumK was observed during the GumK/UDP-GlcA molecular dynamics (MD) simulations. Understanding the underlying catalytic mechanisms of these enzymes and determining their specific contacts with substrates could lead to the development of strategies for their exploitation as unique synthetic catalysts for the generation of modified unnatural polysaccharide variants with potential applications (Nakahara *et al.*, 2006; Choi *et al.*, 2012)

Materials and methods

General procedures and materials

UDP-GlcA was purchased from Sigma-Aldrich (Buenos Aires, Argentina). UDP-[U-14C]GlcA (310 Ci/mol) was prepared by the Sugar-Nucleotide Facility of the Leloir Institute. The proteins were treated with denaturing buffer (100 mM Tris–HCl, 10 M Urea, 2% SDS,

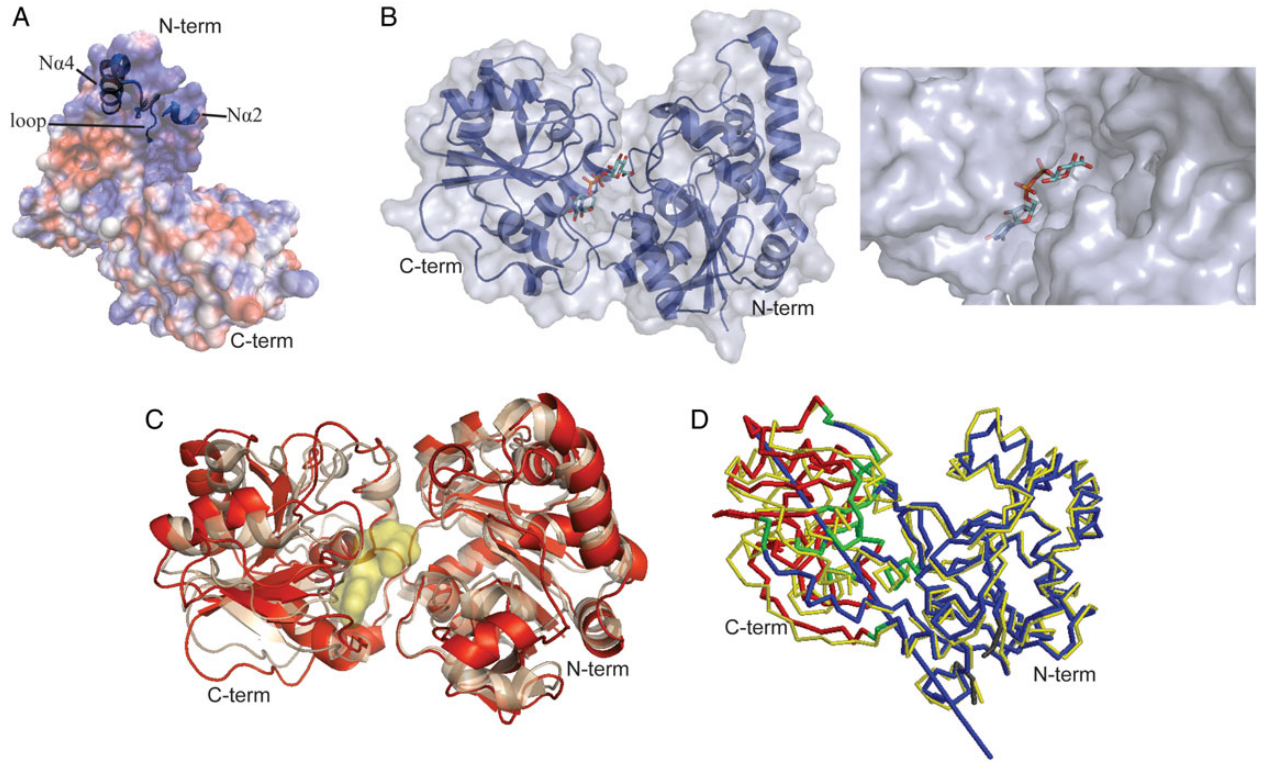

Fig. 1 Modeling and MD of the GumK/UDP-GlcA complex. (**A**) Electrostatic surface potential of GumK (blue, positive; red, negative). The putative regions involved in membrane binding are depicted as cartoons. (**B**) Initial structure for the MD of GumK complexed with UDP-GlcA, obtained by docking. The right image shows the ligand in the cleft, demonstrating the solvent availability of the GlcA portion of the ligand. (**C**) Structural alignment of the crystal structure of GumK (transparent pink) with the representative GumK/UDP-GlcA structure obtained during MD simulations (opaque red). The location of UDP-GlcA is shown as a yellow transparent surface. (**D**) DynDom alignment of the same structures shown in (C); the arrow represents the interdomain screw axis, and the residues are colored based on the degree of rotation of the residue, either with the rotating domain (green) or without it (red). In every panel, the domains are denoted as N- and C-term for clarity.

pH 8.2) and then separated through 10% SDS–PAGE, followed by either Coomassie Blue staining or transfer to PVDF membranes for immunoblot analysis. The protein concentration was determined via the Bradford method (Bradford, 1976). *Escherichia coli* cells were grown in Luria-Bertani (LB) broth (Sambrook *et al.*, 1989) at 37°C (unless otherwise indicated) with shaking at 200 rpm. *Xanthomonas campestris* cells were grown in YM medium (Harding *et al.*, 1993) or in modified XOL medium (Barreras *et al.*, 2004) at 28°C with shaking at 200 rpm.

Substrate modeling and MD simulations

The models of docking and MDs were prepared from the experimental structures of apo-GumK and the GumK/UDP complex (PDB ID: 2HY7 and 2Q6V, respectively). We used the AMBER99 force field for protein residues and nucleotides and the GLYCAM06 force field for carbohydrates (Wang *et al.*, 2004; Kirschner *et al.*, 2008). The structures were protonated and solvated using the tleap tool from the Amber package (Case *et al.*, 2008). Solvation was performed with a simple model of explicit water TIP3P (Jorgensen *et al.*, 1983). Each system underwent a 1000-step minimization via a conjugate gradient method. The final structures were subjected to 120 ps of dynamics simulations at a constant volume, slowly increasing the temperature to 300 K. To equilibrate the system density, we performed another 80 ps of constant-pressure MD. The temperature and pressure were kept constant using a Berendsen thermostat and barostat, respectively. Finally, at least 40 ns of production MD simulations was performed. All of the simulations were performed using periodic boundary conditions and Ewald sums to treat long-range electrostatics, as implemented in Amber.

For the charge parameterization of ligand molecules, a protocol similar to that used for other residues was implemented (Petruk *et al.*, 2009, 2012). The partial charges were RESP charges computed using the Hartree–Fock method and the 6-31G* basis set atoms (Wang *et al.*, 2000). To dock the GlcA portion into GumK/UDP complex, we used our recently developed bias docking protocol, which shows significant improvement for the proper docking of carbohydrates (Gauto *et al.*, 2013; Modenutti *et al.*, 2015). The meaningful Autodock results were carefully examined based on its stereochemical relevance. The sugar analogs were constructed from the GlcA model.

The relative domain rotation was analyzed with DynDom (http://fizz.cmp.uea.ac.uk/dyndom/) (Lee *et al.*, 2003; Poornam *et al.*, 2009). DynDom allows visualization of relative domain motion between two structures. The algorithm defines hinge axis. Axes can be parallel (twist axis) or perpendicular (closure axis) to the axis joining the center of mass of both domains. The percentage of closure is defined as the square of the projection of the hinge axis on the closure axis, being 0% a pure twist motion and 100% a pure closure motion. The percentages are not directly related to a magnitude of closure.

Protein purification

Protein expressed from the plasmid pETHisKC was purified as previously described, obtaining purified GumK in buffer Tris–HCl 20 mM, 400 mM NaCl, 0.05% Triton X-100, pH 8.0 (Barreras *et al.*, 2004). For the biophysical and biochemical assays, to avoid GumK aggregation upon UDP-GlcA addition, a Superdex200 step was performed using a buffer consisting of 400 mM NaCl, 0.05% Triton X-100,

5% glycerol and 25 mM phosphate buffer, pH 8.0. Purified GumK was concentrated to the desired concentration through ultrafiltration and then maintained at 4°C until use. The activity of GumK was tested as described by Barreras *et al.* (Barreras *et al.*, 2004).

Site-directed mutagenesis and mutant analyses

A deletion mutant was obtained through overlapping PCR, with two segments, designated A and B, being generated in the first step. The PCR fragments were amplified from the pETHisKC template using the primers 5'-GACACGGCATATGAGCGTCTCTC-3′ (NdeI site underlined) and 5′GCATATCTCCGCTGTATCGCAACGAAAAAAA AC-3′ for fragment A and the primers 5'CGGGATCCTCAGTGGT GGTGGTGGTGGTG-3′ (BamHI site underlined) and 5′CGATACA GCGGAGATATGCGCCTGCCGCTG-3′ for fragment B. Then, both of the fragments were annealed and extended to obtain a single fragment with the desired deletion. The entire fragment was digested and cloned into the corresponding sites of the pET22b(+) vector (Novagen). Amino acid substitutions were introduced into the cloned *gumK* gene using the QuikChange Site-Directed Mutagenesis Kit (Stratagene) with the primers 5′GCGCATATCTCCCTGCATGTT GGAGAGATTGCTGTATCGCAACG-3′ and 5′CGTTGCGATACA GCAATCTCTCCAACATGCAG-3′ for the R55N/R58N/K60Q substitutions and 5′-GCAGGCGCATATCTCCCTTCGAGCGGGAGC TTCTGCTGTATCGCAACG-3′ and 5′-CGTTGCGATACAGCAGAA GCTCCCGCTCGAAGGGAGATATGCGCCTGC-3′ for L56S/M59S.

For *in vivo* and *in vitro* complementation assays, the ORFs of the mutated *gumK* sequences were cloned into the wide-host-range plasmid pBBRprom under the control of the *gum* operon promoter (Barreras *et al.*, 2008). The correct sequences of the constructs were corroborated through sequencing. Protein expression in the complemented strains was verified through immunoblotting using polyclonal antibodies raised against GumK (Barreras *et al.*, 2004).

For subcellular fractionation, XcK cells complemented with pBBRprom carrying mutated *gumK* were grown to the stationary phase and treated as described in Salinas *et al.* (Salinas *et al.*, 2011). Xanthan production in the XcFC2- and XcK-derived strains (grown on XOL-modified medium for 72 h) was quantified by the cetylpyridinium chloride polysaccharide precipitation method (Barreras *et al.*, 2008).

Turbidity assays

Turbidity was studied by monitoring the absorbance at 350 nm for 60 min at 25°C in a Jasco V-530 UV/Vis spectrophotometer, using a cuvette with a 1 cm path length. GumK was present at a concentration of 10 μM, and when necessary, the indicated substrates were added in small volumes (<2%), to a final concentration of 10, 20 or 50 μM. The time that elapsed between the addition of the ligand and the beginning of measurements was ∼15 s.

Limited proteolysis

A sample of 80 μM GumK (wild-type or substituted) was pre-incubated with 1 mM UDP-GlcA, UDP, UDP-Glc or UDP-GalA or with storage buffer for 5 min at 20°C. The reactions were initiated with the addition of trypsin at a mass ratio of 1:200 in a final volume of 100 μl at 20°C. Aliquots of 10 μl were taken at the indicated times, and the reaction was stopped by incubating the sample with one volume of denaturing buffer supplemented with 2 mM PMSF for 10 min at 100°C. The samples were then stored at −80°C until use. Next, 10 μg of the samples was loaded onto 10% SDS–PAGE gels and stained with Coomassie Blue or transferred to PVDF membranes for N-terminal sequencing via the Edman method (Edman, 1950). The transferred bands were stained with 0.2% Red Ponceau S and sequenced in an Applied Biosystems model 477 sequencer by the Protein and Peptide service (LANAIS-PRO, University of Buenos Aires).

Circular dichroism and fluorescence measurements

Circular dichroism (CD) measurements were performed in a Jasco J-815 spectropolarimeter (Jasco, Japan). Measurements were conducted in a 0.1 cm path length quartz cuvette (Hellma Analytics, Müllheim, Germany) at a scanning speed of 100 nm/min, with a bandwidth of 1 nm and an average response time of 4 s. For far- and near-UV CD measurements, we used GumK at concentrations of 10 and 80 μM, respectively, at 20°C. The temperature was maintained within a range of ±0.1°C using a Peltier thermostat. For the near-UV CD spectra, GumK was incubated with 100 μM UDP-GlcA. For the far-UV CD spectra, GumK was titrated with UDP, UDP-GlcA, UDP-GalA or UDP-Glc, which were added in small volumes (<2%), to a final concentration of 533 μM for UDP-GlcA or 400 μM for the other ligands. The resultant spectra were an average of six measurements. All of the spectra were corrected for the solvent contribution.

The fluorescence emission spectra were measured with a Jasco FP 6500 fluorometer (Jasco, Japan) equipped with a Peltier thermostat set at 20 ± 0.1°C. The fluorescence emission spectra of 80 μM GumK were recorded after excitation of the samples at 295 or 229 nm. The samples were titrated with UDP or nucleotide sugars, which were added in small volumes (<2%), as in the near-UV CD titrations. The resultant spectra were an average of at least three measurements. The measured fluorescence intensities were analyzed and normalized with GraphPad Prism 5.03 (GraphPad Software, La Jolla, CA, USA, www.graphpad.com).

Results

Gumk/UDP-GlcA complex modeling

As mentioned above, the position of the GlcA portion of UDP-GlcA was not resolved by crystallography, most likely due to the molecular motion of the sugar moiety in the absence of the acceptor substrate (Barreras *et al.*, 2008). To investigate the location of the full ligand, we employed molecular docking techniques to construct a GumK/UDP-GlcA model (Fig. 1B) using the crystallographic structure of GumK/UDP and several structures of GumK/UDP obtained from MD simulations as starting points (Gauto *et al.*, 2013; Modenutti *et al.*, 2015). To analyze the stability and dynamic behavior of the obtained model, we performed 40 ns of MD simulations of the GumK/UDP-GlcA system. As controls, we also performed MD of apo GumK and GumK/UDP. These controls systems maintain similar representative structures during equilibrated MDs, indicating that UDP binding do not affect GumK dynamic, at least in our MD setting (Supplementary Fig. S1). When the representative structure of the equilibrated dynamics was compared with the crystal structure or with the MD representative structures of the control systems, we observed that the presence of the complete donor induces a slight interdomain movement in GumK, with no change in the secondary structure of GumK being observed (Fig. 1C). This result is in agreement with the failure of obtaining the structure of GumK/UDP-GlcA structure in soaking experiments because this type of movement cannot occur in crystals. Using the automated DynDom program (Lee *et al.*, 2003), which analyzes conformational changes, hinge axes and amino acid residues involved in the hinge bending between two structures, we obtained a closure percentage of 39.6%, a rotation

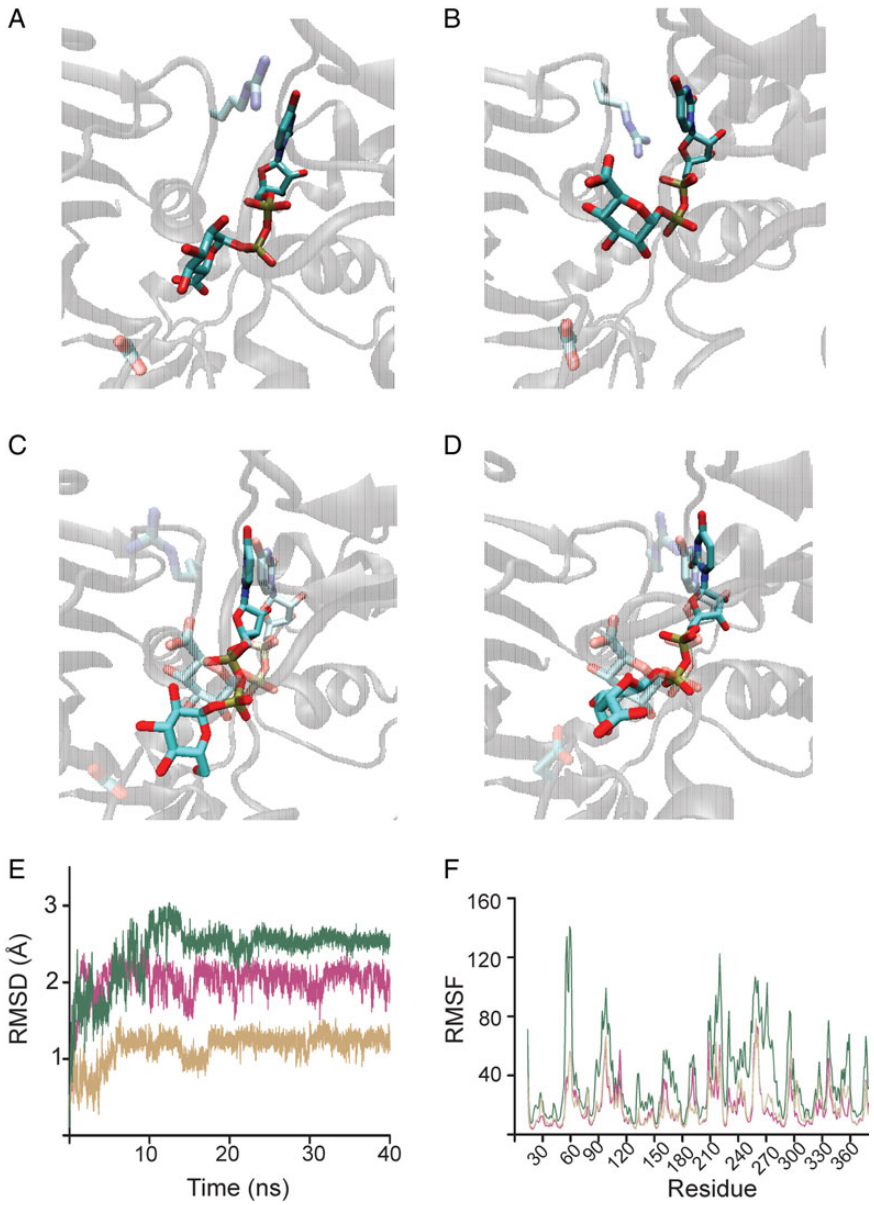

Fig. 2 Structures of GumK and sugar nucleotides after MD. (**A**) Initial position of UDP-GlcA before MD. Representative structure obtained after MD simulations of UDP-GlcA (**B**), UDP-Glc (**C**) and UDP-GalA (**D**). In (A–D), the residues R29 and D157 corresponding to each GumK conformation are shown with a transparent stick. In (C) and (D), the representative structure of UDP-GlcA is shown with a transparent stick for comparison. (**E**) RMSD over time for UDP-GlcA (green), UDP-GalA (violet) and UDP-Glc (brown) during the simulations. (**F**) RMSF of GumK amino acid residues during simulations with a ligand. The same color code employed in (E) is used.

angle of 20.1° and a translation of 0.4 Å, for GumK/UDP-GlcA with respect to the crystallographic structure of GumK. Taking into account the definition of closure percentage, the result suggests the predominance of an interdomain twist motion rather than pure closure (see the Materials and Methods section and references for a description of the method) (Hayward and Berendsen, 1998) (Fig. 1D).

In addition, during the MD simulations, we observed rearrangement of the GlcA residue, exposing its C1′ atom directly to the solvent in the GumK cleft (Fig. 2A and B). The location of the sugar and the relaxation of the structure result in new interactions involving residues of both domains (Table I). A major rearrangement of residues was observed at R29. In the crystallographic structure of GumK, R29 is located at the cleft and is oriented toward the solvent, far from the active site. During the GumK/UDP-GlcA MD simulations, R29 rotated, creating electrostatic interactions with the phosphate and carboxylate groups of UDP and GlcA, respectively. A point substitution changing R29 to alanine was generated, and this protein was expressed in *trans* in the *X.campestris gumK*- mutant strain (XcK). The expression of GumKR29A led to complete restoration of xanthan production by the XcK strain (not shown); thus, the interaction of R29 with UDP-GlcA is not essential for the catalysis mechanism, because the GumKR29 maintain activity. In our previous work (Barreras *et al.*, 2008), we performed kinetic analysis of activity for GumK substituted on residues involved in UDP-crystal contacts and we observed that none of the substitutions led to activity loss. Then, only a substitution on a catalytic and essential residue will avoid activity. In this sense, we reinforce the hypothesis that none residue is in itself essential for ligand binding, rather the biochemical characteristics of the pocket seems

Table I. Atomic interactions within GumK residues and modeled ligands

GumK residues	H-bond distance (Å)		
	UDP-GlcA	UDP-Glc	UDP-GalA
R29/NH2	GlcA O′P (2.88)	–	–
R29/NH2	α-phosphate O2A (2.81)	–	–
R29/NH1	α-phosphate O2A (3.19)	–	–
D157/OD1	–	–	GalA O3′ (2.68)
D157/OD2	–	–	GalA O4′ (2.69)
S230/OG	α-phosphate O1A (2.67)	–	β-phosphate O3B (2.88)
S230/OG	–	–	α-phosphate O2A (2.78)
S230/N	–	–	α-phosphate O1A (2.70)
M273/O	Uracil N3 (2.59)	Uracil N3 (2.86)	Uracil N3 (2.83)
M273/N		Uracil O4 (3.03)	Uracil O4 (2.90)
H275/NE2	Ribose O3′ (3.02)	–	–
H275/ND1	–	Ribose O2′ (2.82)	–
T278/OG1	Uracil O2 (2.64)	–	–
S304/OG	–	Glc O6′ (2.61)	–
S305/OG	β-phosphate O2B (2.59)	β-phosphate O1B (2.88)	β-phosphate O1B (2.55)
K307/N	α-phosphate O3A (3.08)	–	–
K307/NZ	–	α-phosphate O1A (2.90)	α-phosphate O1A (2.70)
K307/NZ	–	β-phosphate O2B (2.83)	β-phosphate O2B (2.94)
M306/N	β-phosphate O1B (2.87)	β-phosphate O1B (2.85)	β-phosphate O1B (2.85)
Q310/OE1	–	Ribose O3′ (2.86)	Ribose O3′ (2.90)
Q310/OE1	–	–	Ribose O2′ (2.68)
Q310/NE2	–	Ribose O2′ (2.83)	–

to determine binding. A sequence alignment of 30 members of the family GT-70 shows, as expected, that conserved residues are located principally, but not only, at C-terminal domain and at the hinge region (Supplementary Fig. S2A). For example, the residues R29, D157, K307 and S304 are conserved among these members. The location of all the conserved residues onto GumK structure suggests a complex network of residues involved in UDP-GlcA binding (Supplementary Fig. S2B). R29, and other interacting-residues, may account for the transient stability of the ligand, participating in the arrangement of its conformation for further catalysis.

Modeling of GumK with UDP-GlcA homologs

Previous results showed that GumK is not able to use related sugar nucleotides, such as UDP-glucose (UDP-Glc) or UDP-galacturonic acid (UDP-GalA), as substrates (unpublished data). To understand this high specificity, we modeled these UDP-GlcA analogues using the GumK/UDP-GlcA docking model as a template. Then, we performed MD simulations (Fig. 2C and D). The representative structure of the MD simulations showed that the O3 and O4 of GalA are stabilized preferentially with the D157 residue, while the only H-bond involved in Glc stabilization was located between O6 and S304. The H-bonds between GumK residues and ligands are described in Table I. In contrast, none of the analogues induced the movement of R29 observed within the GumK/UDP-GlcA dynamics. UDP-GalA and UDP-Glc do not experience torsion during MD simulations, as judged through a visual inspection of the MD structures, and they did not significantly vary in their overall conformation during the dynamics simulations, as judged by RMSD analyses performed over time (Fig. 2E). Inter-domain movement of GumK was observed in the presence of the analogs as well, but the significance and the trend of the inter-domain movement was different from that observed in the GumK/UDP-GlcA MD (Supplementary Fig. S1). DynDom analyses showed that no significant interdomain movement occurred upon UDP-GalA binding, and with UDP-Glc, an interdomain closure percentage of 98% was detected, corresponding to a relative closure motion of the domains rather than twist motion (Hayward and Berendsen, 1998). In competitive enzymatic assays, we observed no interference with GumK activity in the presence of UDP-GalA or UDP-Glc (not shown). Taken together, the structural similarity of the analogs and their interactions, their failure to inhibit GumK competitively and the lack of significant movement appear to indicate that GumK specificity is linked to this conformational change.

UDP-GlcA binding triggers fluctuation of the putative membrane-binding domain

The analysis of amino acid residue fluctuations during equilibrated dynamics, as determined by their root mean square fluctuation (RMSF), revealed two regions with increased motility in GumK/UDP-GlcA (Fig. 2F). Some residues in the 240–280 amino acid region are involved in UDP binding; thus, fluctuation in this region may indicate the rearrangement of residues to properly accommodate UDP-GlcA during its torsion. Moreover, DynDom recognizes these residues as bending residues. Interestingly, there is also a fluctuation in the R56-K60 amino acid region corresponding to the Nα2 helix. This α-helix is proposed to be one of the secondary structures at the N-termini that are involved in membrane and/or acceptor binding. As can be observed in the GumK structure, the residues located at Nα2 helix have no contact with the donor substrate and are more than 20 Å distant from the active site. To analyze the relative importance of Nα2 residues, we generated point substitutions at various residues of this structure and analyzed its functionality through complementation of the XcK strain. The protein with the R55N/R58N/K60Q substitutions in basic residues maintains its membrane location, as observed via the subcellular fractionation of XcK expressing the substituted protein in *trans*. Permeabilized XcK cells expressing the substituted protein *in trans* were prepared as previously described, and the cells were then incubated with nucleotide sugars to analyze the obtained product. During these incubations, the obtained reaction product was

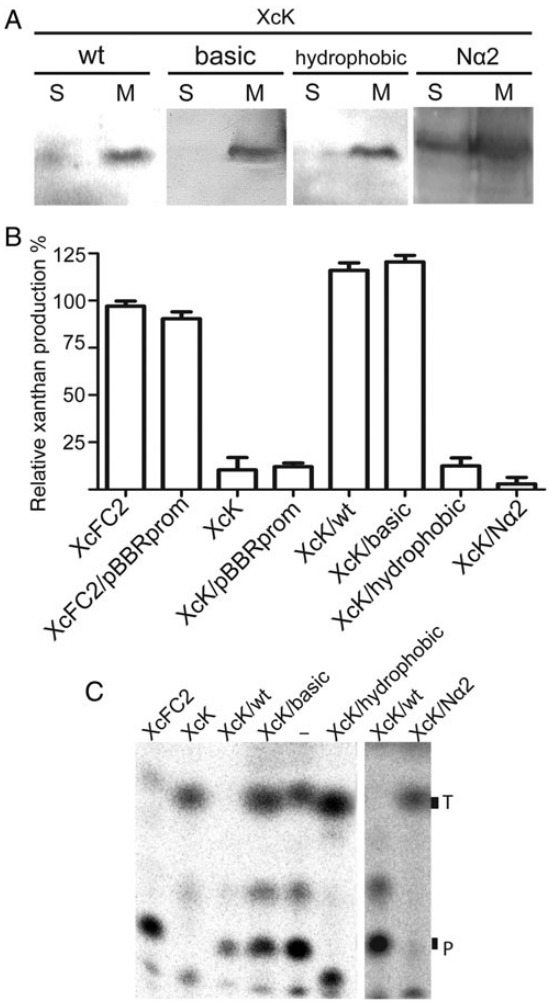

Fig. 3 Analysis of putative membrane-binding region. (**A**) The localization of GumK variants expressed *in trans* in a XcK strain was analyzed via western blotting of subcellular fractions (S, soluble fraction; M, membrane fraction). (**B**) The functionality of the GumK variants was assessed by measuring xanthan production in the complemented strains. As controls, we used the XcFC2 wild-type strain and XcK, and both of which containing the empty pBBRProm vector. (**C**) The *in vitro* activity of the GumK variants was measured by permeabilized cells incubation and analyzed via TLC using the same controls as in (B). T and P indicate the positions of the trisaccharide and pentasaccharide, respectively. The line marked as (–) corresponds to a substitution that is not described in this work. The analysis of the product of XcK/Nα2 was performed in a parallel TLC analysis. GumK variants: Wt, wild-type; basic, R55N/R58N/K60Q; hydrophobic, L56S/M59S.

Lip-PP-pentasaccharide, as expected for wild-type activity. Thus, the substitution in these basic residues did not affect *in vitro* activity in permeabilized XcK cells. In contrast, the L56S/M59S substitution, with alterations of hydrophobic residues, is also directed to membranes but lacks *in vitro* and *in vivo* activity, as judged based on the absence of the Lip-PP-pentasaccharide product and xanthan production, respectively. A similar result was obtained with the Δ(Nα2) variant, carrying a deletion of the entire helix (R55-K60). Based on the correct subcellular locations of these proteins, their absence of activity is likely due to an inability to properly change their conformation and/or effectively bind their acceptor substrate. The analyses of the subcellular locations and the *in vitro* and *in vivo* activities of the GumK variants are shown in Fig. 3. As we stated previously, this N-terminal region may be involved in both acceptor and membrane binding.

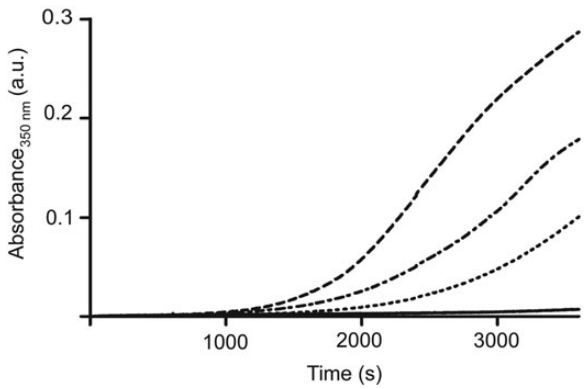

Fig. 4 UDP-GlcA induced aggregation of GumK in Tris buffer. Turbidity at 350 nm versus time for 10 μM purified GumK—using the protocol described in Barreras *et al.* (Barreras *et al.*, 2004)—, in the presence of 10 μM (short dashed), 20 μM (dot dashed) or 50 μM (large dashed) UDP-GlcA. The continuous line represents the absorbance in arbitrary units (a.u.) of a sample of GumK purified using the new protocol, in the presence of 50 μM UDP-GlcA.

Then, the mechanism of conformation changes in this region must be nearly specific of each membrane-bound GT, because the variety of acceptors and membranes that exists in nature.

Ligand binding triggers conformational change

As described in the Introduction section, several examples of conformational changes in GTs were observed upon donor binding as part of the enzymatic mechanism (Vetting *et al.*, 2008; Giganti *et al.*, 2013; Albesa-Jove *et al.*, 2014). For GumK, the MD analyses described in this work may suggest the presence of a greater conformational change triggered by UDP-GlcA binding. To test this hypothesis, we applied several biophysical techniques. In preliminary assays, we found that a solution containing recombinant GumK, which was purified as previously described (Barreras *et al.*, 2004), becomes turbid to the naked eye after the addition of a 3-fold molar excess of UDP-GlcA. To observe this process qualitatively, we measured turbidity as a function of the absorbance at 350 nm. As shown in Fig. 4, the rate of turbidity in the GumK solution increased in a UDP-GlcA-dependent manner. In addition, the absorbance at 350 nm in the presence of UDP-Glc and UDP-GalA was not altered, even at similar concentrations to those assayed for UDP-GlcA (not shown). These results suggest that there is a conformational change upon ligand binding that makes GumK insoluble in the buffer employed in these assays. To perform further experiments, we required a stable solution of GumK. Several buffer systems were tested in the presence of UDP-GlcA to determine conditions in which no aggregation was detected. In the new buffering system, Tris–HCl was replaced with phosphate buffer and 5% glycerol was added; further details of the purification protocol are provided in the Materials and methods section. GumK purified with this new buffer maintained its GT activity, showed hydrolytic activity against UDP-GlcA in the absence of an acceptor substrate (Supplementary Fig. S3, top), and was maintained in solution during the interaction with the ligand (Fig. 4, continuous line).

Our next approach for studying ligand-induced conformational changes in GumK was an *in vitro* limited trypsin proteolysis assay. This technique is widely used to demonstrate changes in protein structure because a more exposed protein region will be more susceptible to protease digestion (Fontana *et al.*, 2004). In particular, trypsin cleaves peptides on the C-terminal side of Lys and Arg amino acid residues, except when a Pro is present on the C-terminal side. As shown in

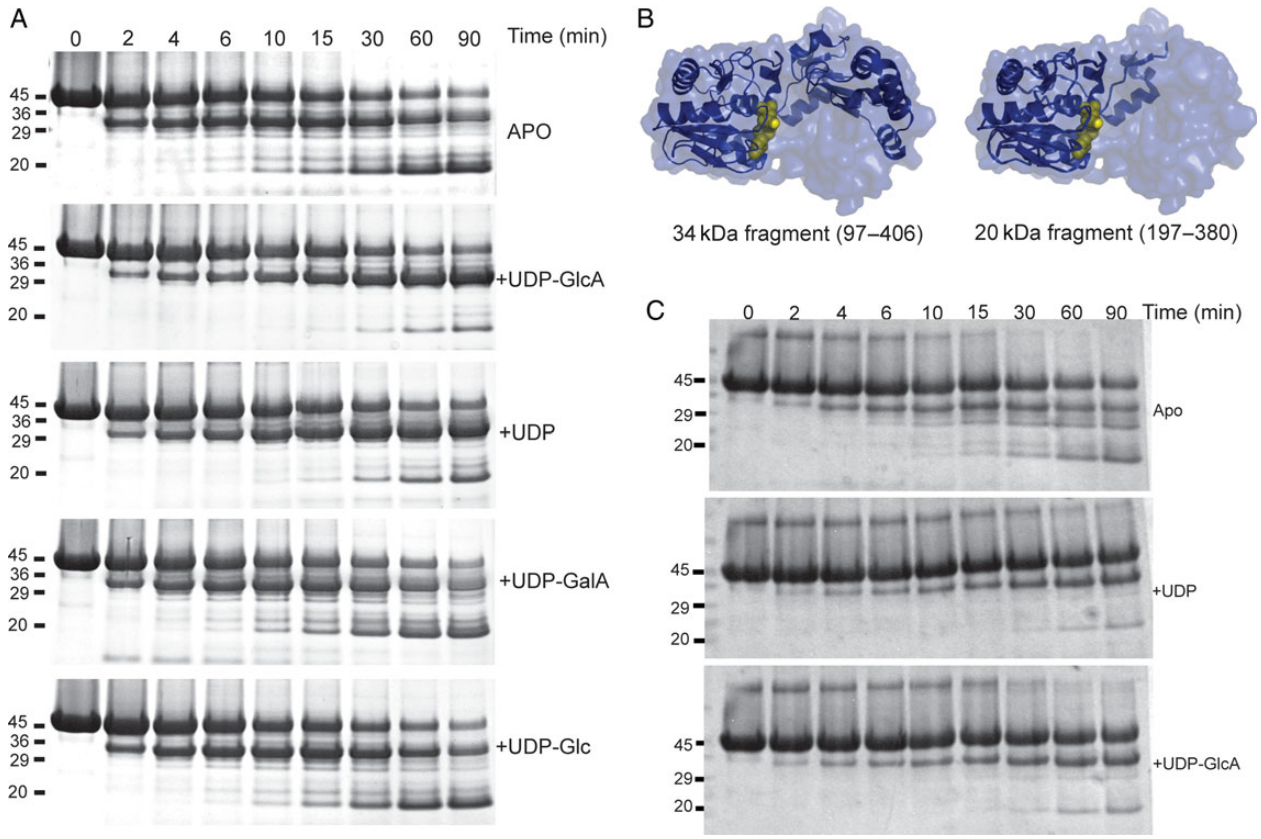

Fig. 5 Controlled proteolysis of GumK. (**A**) Time course of the proteolysis (with trypsin) of wild-type apo-GumK or GumK incubated with UDP-GlcA, UDP, UDP-GalA or UDP-Glc. (**B**) Representation of the two main digestion fragments. The surface of the complete GumK protein is transparent, and the fragment is imposed in a cartoon representation. The position of UDP in the crystal (PDB ID: 2Q6 V) is shown as yellow spheres. (**C**) Time course of the proteolysis (with trypsin) of GumKD157A in its apo form or in the presence of UDP or UDP-GlcA.

Fig. 5A, GumK presented different kinetics of digestion when UDP or UDP-GlcA was present, while the behavior of GumK in the presence of UDP-Glc or UDP-GalA was similar to that of apo GumK. In every case, the identity of the fragments produced via digestion was the same, but the bands were released at different times. Thus, GumK presented different digestion kinetics when UDP or UDP-GlcA was present. The N-terminal sequence of the principal fragments was determined through Edman sequencing. The ~34 kDa fragment that was released first corresponds to the 97–406 amino acid segment (Fig. 5B). This segment contains the complete C-terminal domain and a fraction of the N-terminal domain. The cleavage site that generated this ~34 kDa fragment is located between the loop and Nα4, which is proposed to constitute part of the membrane-interacting region. The fragment was released with an apparent difference in the digestion yield being observed in GumK/UDP and GumK/UDP-GlcA mixes, suggesting an overall stabilization of the GumK structure in these complexes and a change in the exposure of residues exposed at the cleavage site. Moreover, based on the observed band intensities, this fragment was noticeably protected from proteolysis in the presence of UDP-GlcA or UDP. Ultimately, the fragment was principally digested into a ~20 kDa fragment (Fig. 5B). This fragment, corresponding to residues 197–406, is the complete C-terminal domain. Taking into account these two fragments, the presence of UDP-GlcA and UDP resulted in a change in at least the exposure or accessibility of basic residues of the interdomain linker region and in the putative membrane-binding region around R96.

As mentioned above, GumK is able to hydrolyze UDP-GlcA *in vitro*. We performed limited digestion assays with the non-hydrolytic GumKD157A to study whether the hydrolysis mechanism and the resulting UDP release also affected the proteolysis kinetics or if the observed results are only due to the binding process. We previously showed that this variant is not active, is unable to hydrolyze UDP-GlcA and exhibits an indistinguishable structure from that of wild-type GumK (Supplementary Fig. S3, bottom, and Barreras *et al.*, 2008). In this case, we observed the same digestion pattern as was described for wild-type GumK (Fig. 5C).

Behavior of the tertiary structure of apo-GumK and donor substrate-bound forms

To further study the existence of conformational changes in the GumK structure upon the addition of the donor substrate, we collected CD measurements. We were able to measure a reliable CD signal only within the range of 210–260 nm for far-UV because at shorter wavelengths, the noise was high. Therefore, no estimate of the secondary structure content was obtained. Even so, we observed no significant changes in the far-UV CD upon the addition of UDP-GlcA to GumK (Fig. 6A), suggesting an absence of secondary structure rearrangement. However, titration monitored by near-UV CD showed differential spectra depending on the UDP-GlcA concentration (Fig. 6B). There was a decrease in the ~260 nm signal and a shift in the wavelength such that the peak occurred in the absence of UDP-GlcA. The addition of UDP, UDP-GalA or UDP-Glc did not alter the near-UV CD spectra with respect

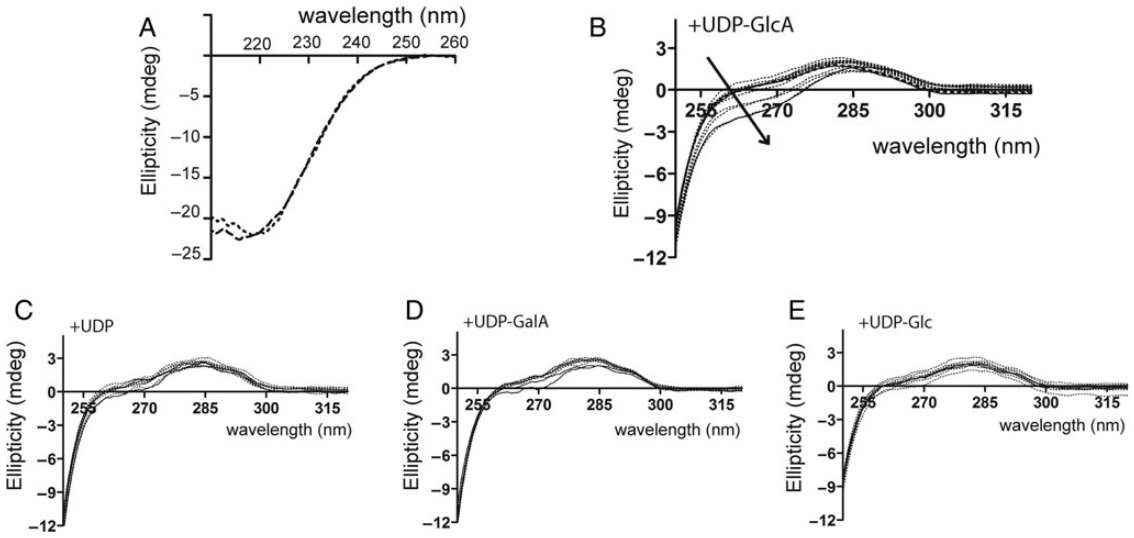

Fig. 6 CD analysis of GumK. (**A**) Far-UV CD signal of GumK (dashed line) and GumK with UDP-GlcA (dotted line). Near-UV CD signal of the titration of GumK with UDP-GlcA (**B**), UDP (**C**), UDP-GalA (**D**) and UDP-Glc (**E**). The initial (apo GumK) and final condition (>400 μM ligand) are depicted as full lines. Intermediate concentrations are depicted as dotted lines. The arrow in (B) indicates the direction of the increase in the UDP-GlcA concentration.

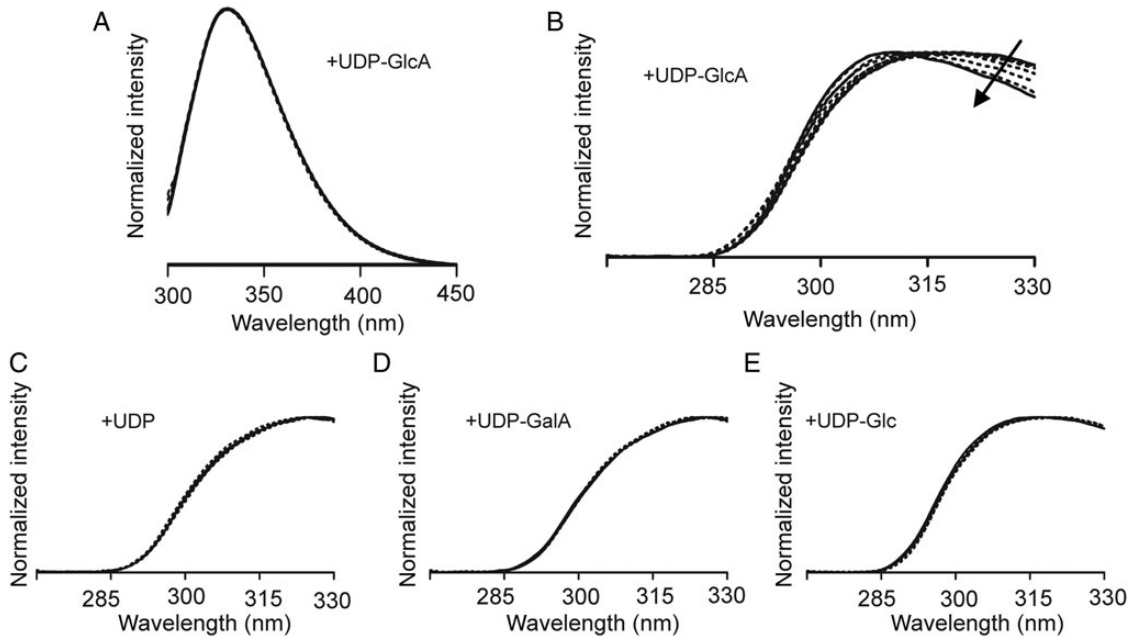

Fig. 7 Fluorescence spectra of GumK and Triton X-100. (**A**) Normalized intensity of intrinsic tryptophan fluorescence during the titration of GumK with UDP-GlcA. No change in the wavelength of maximum emission was detected. Normalized intensity of fluorescence after the excitation of mainly Triton X-100 molecules at 229 nm during the titration of GumK with UDP-GlcA (**B**), UDP (**C**), UDP-GalA (**D**) or UDP-Glc (**E**). The lines code is the same as in Fig. 6. The arrow in (B) indicates the direction of the increase in the UDP-GlcA concentration. The spectra are normalized to reduce variations in intensity due to titration.

to those of apo-GumK (Fig. 6C–E). Based on near- and far-UV CD measurements, we detected no improvement in the thermal stability of GumK in the presence of UDP-GlcA (Supplementary Fig. S4).

Additionally, we studied the fluorescence emission spectra after the excitation of tryptophan residues at 295 nm. Figure 7A shows a normalized representative assay of GumK titration with UDP-GlcA. There was no change in the wavelength of the maximum emission. Taking into account the hypothesis of hydrophobic residue exposure upon UDP-GlcA binding, we excited the sample at 229 nm, which is the excitation wavelength of Triton X-100 molecules, detergent employed for the purification of GumK. At this excitation wavelength, we expected null or negligible intrinsic protein fluorescence emission. In the obtained emission spectra, we observed a shift in the wavelength of maximum emission only in the presence of UDP-GlcA (Fig. 7B–E). The observed blue shift may suggest an increase in the hydrophobic environment of Triton X-100 molecules. To determine whether the observations were related to discrete aggregation, we performed chemical cross-linking using DSP with up to a 50× molar excess of UDP-GlcA at two different temperatures (Supplementary Fig. S5). Moreover, we performed size exclusion chromatography after incubation (not shown). In every case, no

aggregation was detected. Also, the change in the signal in the near-UV CD upon thermal denaturation and the consequent aggregation were quite different from those obtained as a function of UDP-GlcA (see Fig. 6B and Supplementary Fig. S4). Therefore, the results suggest the existence of a conformational change in the tertiary structure of GumK, most likely altering the exposure of hydrophobic residues.

Discussion

The results presented herein suggest that GumK presents a conformational change upon donor substrate binding that may be partially responsible for the donor substrate selectivity of GumK. This type of event has been demonstrated in other GTs, and the type and extent of changes that occur appear to indicate the differences between proteins from the same structural superfamily (Vetting *et al.*, 2008; Chan *et al.*, 2012; Giganti *et al.*, 2013; Albesa-Jove *et al.*, 2014). Despite these examples, little is known about GT structure and mechanisms. Analyzing the data in the CAZy database, we found that more than 800 00 out of 220 000 putative GT belongs to inverting GT-B clan. At this moment, there are known only 12 structures of these GTs complexed with donor sugar nucleotides. It means that <0.2% of putative inverting GT-B are described in terms of structural interaction with donor substrate. These 12 structures are distributed in only four families (GT 1, 2, 28, 41), and only eight present UDP-derived sugar nucleotides. The *E. coli* chondroitin polymerase KfoC is the only inverting GT-B crystallized with UDP-GlcA. KfoC lacks a membrane-interacting domain and it seems to form complex with other membrane proteins (Ninomiya *et al.*, 2002). The only membrane-associated inverting GT-B member crystallized with its UDP-derived donor substrates is MurG (Ha *et al.*, 2000). Taking into account these numbers, it is not correct to do generalizations. Much effort must be performed to gain information about GTs structure–mechanism relationship. For GumK, the existence of a conformational change may explain our difficulties in trapping the complex via either co-crystallization or soaking of GumK crystals with UDP-GlcA. Here, several experimental approaches, together with docking and MD simulations, provide further evidence supporting ligand-induced conformational change.

We propose a model of UDP-GlcA located in the GumK cleft, which was created based on docking and a critical inspection of the GumK structure. MD simulations of the sugar nucleotides UDP-GlcA, UDP-Glc and UDP-GalA bound to GumK suggest that differential interactions may be responsible for the observed specificity because UDP-GlcA exhibited altered torsion, whereas the analogs did not. The torsion of UDP-GlcA exposes its GlcA C1′ atom to the solvent; thus, transferase catalysis may be more accessible. Taking into account our previous study, we propose that the overall interactions between GumK and its ligands and the dynamics of nucleotide sugars and GumK residues are concerted events that account for the observed specificity. During MD, the protein suffers global movement and local fluctuations at several residues. Nevertheless fluctuations, the residues surrounding UDP-GlcA may suggest the existence of the next stage in the conformation on a large timescale. The most surprising fluctuation was that observed in the non-ligand-interacting region of Nα2. Experimental substitution of hydrophobic (L56S/M59S), but not basic (R55N/R58N/K60Q), residues demonstrated their importance for enzyme activity, although the *in vivo* membrane location was not significantly altered. In addition, the experimental deletion or variation of Nα2 completely abolished enzyme activity, although the protein was correctly membrane located. These results suggest that the fluctuations observed during MD are part of a greater conformational change, most likely with the consequence of accommodating the acceptor substrate and ultimately catalyzing the reaction. In this sense, the insoluble aggregation of GumK upon the binding of UDP-GlcA, as observed in turbidity assays, may be related to the fluctuation and exposure of hydrophobic residues in the N-terminal region, whose interaction would provoke the aggregation and precipitation of GumK molecules. A similar class of mechanism has been observed in other GTs. In particular, MshA suffers a reorientation of domains upon interaction with its donor substrate, through which the acceptor binding site in the N-terminal domain is created (Vetting *et al.*, 2008). The variety of acceptor substrate and membranes that interacts with GTs, and of conformational changes described suggest that the mechanisms of binding and further catalysis are particular of each enzyme.

Despite being fundamental for substrate binding to GumK, the UDP portion is not sufficient for specificity among UDP-sugars. It is clear that GumK requires specifically positioned OH and acid groups to accommodate its donor substrate properly and to catalyze the transfer of monosaccharide to the acceptor substrate. There is no experimental evidence regarding whether GumK effectively binds UDP-Glc or UDP-GalA. Although all of the analogs interact with GumK in our models (at least by force), the consequence of each interaction is different, and UDP-GlcA binding appears to be the only type of binding that is consistent with catalysis.

Limited proteolysis analyses showed that GumK is less sensitive to trypsin when UDP-GlcA or UDP is bound, suggesting that GumK is globally more compact in the presence of UDP-GlcA or UDP. Amine-terminal sequencing of the ~34 and ~20 kDa digestion fragments permitted the identification of at least one region that is affected by UDP-GlcA and UDP binding. Because these fragments appear more slowly in GumK/UDP-GlcA proteolysis reactions, we can conclude that the basic residues in the linker interdomain region and around R96 in the putative membrane-binding region are less exposed compared with the apo protein. Based on comparing the results of experiments using wild-type GumK and the non-hydrolytic GumKD157A as trypsin substrates, we conclude that the hydrolysis of UDP-GlcA does not contribute to the conformational change observed under the analyzed conditions.

The CD experiments showed no change in the overall secondary structure content of the apo and bound forms, as observed based on far-UV CD spectra. We do not exclude the possibility of secondary structure rearrangement that not change the net secondary structure content, as in PimA. PimA suffers both β-strand-to-α-helix and α-helix-to-β-strand transitions comparing apo with GDP-bound form. Using near-UV CD, we observed a change in the spectra only when GumK was titrated with UDP-GlcA. Due to biochemical characteristic of UDP-GlcA, we cannot exclude that the observed changes in CD signal include UDP-GlcA torsion after binding to GumK. Taking all results together, we suggest that the conformational change occurs at the tertiary structure level. As a control for our experiments, taking into account the aggregation observed in the initial trials, we performed cross-linking experiments. In this test, we did not detect aggregation; therefore, we can assume that the observed changes are due only to binding. CD measurements performed in the near- and far UV and fluorescence spectroscopy revealed no improvement in the thermal stability of GumK in the presence of any ligand (partially showed in Supplementary Fig. S4). In contrast, the 'closed' state of PimA (GDP-bound form) showed a higher melting temperature compared with the apo form, thereby indicating increased ligand-mediated stability. Thus, our results contribute to demonstrate the variety of conformational changes found among GTs.

Intrinsic fluorescence upon titration with nucleotide sugars did not show any changes in the maximum emission, indicating that no net

environmental polarity changes are detected by the tryptophan residues of GumK. Studying fluorescence emission after excitation at 229 nm, which is the wavelength of excitation of Triton X-100 molecules, revealed a shift in the emission maximum only when GumK was incubated with UDP-GlcA. The observed blue shift may indicate that the Triton X-100 molecules were sensing a less polar environment. Although these results are not decisive, they reinforce the hypothesis that exposure of hydrophobic residues occurs upon the binding of UDP-GlcA to GumK, in accordance with the turbidity and MD results.

We also show that several residues of C-terminal of members of family GT-70 are conserved, as expected. In spite of we cannot extend the hypothesis of conformational change upon donor binding in all GTs, we suggest that it is probable that it indeed occur in members of family GT-70 because the conservation of residues involved in UDP-GlcA binding.

As a general conclusion, we speculate that UDP-GlcA binding to GumK triggers a change in the GumK tertiary structure, affecting N-terminal hydrophobic residues to generate or improve the lipid-derived acceptor substrate site, while UDP-GlcA accommodates the transfer reaction. In addition to the results presented here, and as example of the complexity of the substrate interactions, we previously showed that a substitution in residue K307 (involved in UDP binding in crystals) has a reduced affinity for both acceptor and donor substrates, even though it only interacts with UDP phosphates (Barreras *et al.*, 2008). Considering all our results, we proposed that protein dynamics are fundamental to the enzymatic activity of GumK.

Supplementary data

Supplementary data are available at *PEDS* online.

Acknowledgements

We thank M. Soledad Malori for her help with protein purification, Diego Gauto for his help with sugar docking, Susana Raffo for UDP-[14C]GlcA preparation and Marta Bravo for his help with DNA sequencing.

Funding

This work was supported by the Agencia Nacional de Promoción Científica y Tecnológica (ANPCyT) (PICT 1/2452) (Argentina) and the Consejo Nacional de Investigaciones Científicas y Técnicas (CONICET) (PIP 399) (Argentina). S.R.S. and M.J. were doctoral fellows of CONICET. A.A.P. and M.I.B. were postdoctoral fellows of CONICET. M.A.M. and L.I. are members of the Investigator Career of CONICET.

References

Albesa-Jove,D., Giganti,D., Jackson,M., Alzari,P.M. and Guerin,M.E. (2014) *Glycobiology*, **24**, 108–124.

Barreras,M., Abdian,P.L. and Ielpi,L. (2004) *Glycobiology*, **14**, 233–241.

Barreras,M., Bianchet,M.A. and Ielpi,L. (2006) *Acta Crystallogr. Sect. F Struct. Biol. Cryst. Commun.*, **62**, 880–883.

Barreras,M., Salinas,S.R., Abdian,P.L., Kampel,M.A. and Ielpi,L. (2008) *J. Biol. Chem.*, **283**, 25027–25035.

Bradford,M.M. (1976) *Anal. Biochem.*, **72**, 248–254.

Breton,C., Fournel-Gigleux,S. and Palcic,M.M. (2012) *Curr. Opin. Struct. Biol.*, **22**, 540–549.

Case,D., Darden,T., Cheatham Iii,T., *et al.* (2008) AMBER 10.

Coutinho,P.M., Deleury,E., Davies,G.J. and Henrissat,B. (2003) *J. Mol. Biol.*, **328**, 307–317.

Chan,P.H., Weissbach,S., Okon,M., Withers,S.G. and McIntosh,L.P. (2012) *Biochemistry*, **51**, 8278–8292.

Choi,S.H., Kim,H.S., Yoon,Y.J., Kim,D.-M. and Lee,E.Y. (2012) *J. Ind. Eng. Chem.*, **18**, 1208–1212.

Edman,P. (1950) *Acta Chem. Scand.*, **4**, 283–293.

Edman,M., Berg,S., Storm,P., Wikstrom,M., Vikstrom,S., Ohman,A. and Wieslander,A. (2003) *J. Biol. Chem.*, **278**, 8420–8428.

Fontana,A., de Laureto,P.P., Spolaore,B., Frare,E., Picotti,P. and Zambonin,M. (2004) *Acta Biochim. Pol.*, **51**, 299–321.

Gauto,D.F., Petruk,A.A., Modenutti,C.P., Blanco,J.I., Di Lella,S. and Marti,M.A. (2013) *Glycobiology*, **23**, 241–258.

Giganti,D., Alegre-Cebollada,J., Urresti,S., *et al.* (2013) *J. Biol. Chem.*, **288**, 29797–29808.

Giganti,D., Albesa-Jove,D., Urresti,S., *et al.* (2015) *Nat. Chem. Biol.*, **11**, 16–18.

Grizot,S., Salem,M., Vongsouthi,V., Durand,L., Moreau,F., Dohi,H., Vincent, S., Escaich,S. and Ducruix,A. (2006) *J. Mol. Biol.*, **363**, 383–394.

Guerin,M.E., Kordulakova,J., Schaeffer,F., Svetlikova,Z., Buschiazzo,A., Giganti,D., Gicquel,B., Mikusova,K., Jackson,M. and Alzari,P.M. (2007) *J. Biol. Chem.*, **282**, 20705–20714.

Ha,S., Walker,D., Shi,Y. and Walker,S. (2000) *Protein Sci.*, **9**, 1045–1052.

Harding,N.E., Raffo,S., Raimondi,A., Cleary,J.M. and Ielpi,L. (1993) *J. Gen. Microbiol.*, **139**, 447–457.

Hayward,S. and Berendsen,H.J.C. (1998) *Prot. Struct. Funct. Bioinform.*, **30**, 144–154.

Henrissat,B., Sulzenbacher,G. and Bourne,Y. (2008) *Curr. Opin. Struct. Biol.*, **18**, 527–533.

Hubbell,W.L., Cafiso,D.S. and Altenbach,C. (2000) *Nat. Struct. Biol.*, **7**, 735–739.

Jorgensen,W.L., Chandrasekhar,J., Madura,J.D., Impey,R.W. and Klein,M.L. (1983) *J. Chem. Phys.*, **79**, 926–935.

Katzen,F., Ferreiro,D.U., Oddo,C.G., Ielmini,M.V., Becker,A., Puhler,A. and Ielpi,L. (1998) *J. Bacteriol.*, **180**, 1607–1617.

Kirschner,K.N., Yongye,A.B., Tschampel,S.M., Gonzalez-Outeirino,J., Daniels, C.R., Foley,B.L. and Woods,R.J. (2008) *J. Comput. Chem.*, **29**, 622–655.

Lairson,L.L., Henrissat,B., Davies,G.J. and Withers,S.G. (2008) *Annu. Rev. Biochem.*, **77**, 521–555.

Lee,R.A., Razaz,M. and Hayward,S. (2003) *Bioinformatics*, **19**, 1290–1291.

Lind,J., Ramo,T., Klement,M.L., Barany-Wallje,E., Epand,R.M., Epand,R.F., Maler,L. and Wieslander,A. (2007) *Biochemistry*, **46**, 5664–5677.

Lombard,V., Golaconda Ramulu,H., Drula,E., Coutinho,P.M. and Henrissat, B. (2014) *Nucleic Acids Res.*, **42**, D490–D495.

McHaourab,H.S., Steed,P.R. and Kazmier,K. (2011) *Structure*, **19**, 1549–1561.

Mittermaier,A.K. and Kay,L.E. (2009) *Trends Biochem. Sci.*, **34**, 601–611.

Modenutti,C., Gauto,D., Radusky,L., Blanco,J., Turjanski,A., Hajos,S. and Marti,M. (2015) *Glycobiology*, **25**, 181–196.

Nakahara,T., Hindsgaul,O., Palcic,M.M. and Nishimura,S.-I. (2006) *Protein Eng. Des. Sel.*, **19**, 571–578.

Ninomiya,T., Sugiura,N., Tawada,A., Sugimoto,K., Watanabe,H. and Kimata, K. (2002) *J. Biol. Chem.*, **277**, 21567–21575.

Petruk,A.A., Marti,M.A. and Alvarez,R.M. (2009) *J. Phys. Chem. B*, **113**, 13357–13364.

Petruk,A.A., Bartesaghi,S., Trujillo,M., Estrin,D.A., Murgida,D., Kalyanaraman, B., Marti,M.A. and Radi,R. (2012) *Arch. Biochem. Biophys.*, **525**, 82–91.

Poornam,G.P., Matsumoto,A., Ishida,H. and Hayward,S. (2009) *Proteins*, **76**, 201–212.

Salinas,S.R., Bianco,M.I., Barreras,M. and Ielpi,L. (2011) *Glycobiology*, **21**, 903–913.

Sambrook,J., Fritsch,E.F. and Maniatis,T. (1989) *Molecular Cloning: A Laboratory Manual*, 2nd edn, Cold Spring Harbor Laboratory Press, New York.

Vetting,M.W., Frantom,P.A. and Blanchard,J.S. (2008) *J. Biol. Chem.*, **283**, 15834–15844.

Wang,J., Cieplak,P. and Kollman,P.A. (2000) *J. Comput. Chem.*, **21**, 1049–1074.

Wang,J., Wolf,R.M., Caldwell,J.W., Kollman,P.A. and Case,D.A. (2004) *J. Comput. Chem.*, **25**, 1157–1174.

Weadge,J.T., Palcic,M.M. and Begley,T.P. (2007) *Wiley Encyclopedia of Chemical Biology*. John Wiley & Sons, Inc., New York.